

Polaronic Variable Range Hopping Mediated Electrical Transport Mechanisms in Ferromagnetic $\text{Pr}_2\text{FeMnO}_6$

Kaipamangalath Aswathi^{1,a}, Manoj Raama Varma^{2,b}

¹ Sensors and Energy Materials Group, Center for Materials for Electronics Technology (CMET), Thrissur, Kerala, India.

² CSIR-National Institute for Interdisciplinary Science and Technology (NIIST), Thiruvananthapuram, Kerala, India.

^a aswathi1444@gmail.com

^b manojraamavarma@gmail.com

Abstract

The electrical transport properties of oxide materials are largely dictated by electron-phonon interactions, which often lead to the formation of polarons, significantly influencing the conduction mechanism. In the case of the ferromagnetic orthorhombic perovskite oxide $\text{Pr}_2\text{FeMnO}_6$, the material exhibits insulating behaviour at room temperature, with a resistivity of approximately $4.1 \times 10^3 \Omega \cdot \text{m}$. As the temperature decreases, the resistivity increases markedly, reaching $73.47 \times 10^3 \Omega \cdot \text{m}$ at 122 K, with a pronounced rise occurring below 160 K. To elucidate the conduction mechanism, the Variable Range Hopping (VRH) model is applied. This model describes electron hopping between non-nearest neighbour sites, which becomes favourable when the thermal energy is insufficient for nearest-neighbour hopping. Instead, electrons preferentially hop to sites with lower potential differences. The temperature dependence of resistivity is well-described by the VRH model, confirming its applicability in this system. In addition to electrical transport, the structural and magnetic properties of $\text{Pr}_2\text{FeMnO}_6$ have also been investigated. Notably, the material exhibits a magnetization reversal at low temperatures, further enriching its magnetic behaviour and potential applications.

Keywords: Conduction mechanisms; Variable range hopping; Sign reversal of Magnetization.

Received 30 January 2025; First Review 19 March 2025; Accepted 01 April 2025.

* Address of correspondence

Kaipamangalath Aswathi
Sensors and Energy Materials Group Center for
Materials for Electronics Technology (CMET),
Thrissur, Kerala, India.

Email: aswathi1444@gmail.com

How to cite this article

Kaipamangalath Aswathi, Manoj Raama Varma, Polaronic Variable Range Hopping Mediated Electrical Transport Mechanisms in Ferromagnetic $\text{Pr}_2\text{FeMnO}_6$, J. Cond. Matt. 2025; 03 (02): 83-88.

Available from:
<https://doi.org/10.61343/jcm.v3i02.125>



Introduction

Perovskite oxides have become a focal point in materials science research because of their exceptional versatility and diverse range of physical properties, including superconductivity, ferroelectricity, magnetoresistance, and catalytic functionality [1, 2]. These properties arise from their characteristic crystal structure, typically represented as, where and are cations of different sizes and is an anion, often oxygen. Substitutions at the sites provide immense tunability in their structural, electronic, and magnetic characteristics, making perovskites ideal candidates for technological applications such as sensors, spintronics, and energy storage devices [3]. Among the various physical properties of perovskite oxides, their electrical transport behavior has been the subject of extensive study. The conduction mechanism in these materials is predominantly governed by the interactions between electrons and phonons, often leading to the formation of polarons. These quasiparticles, arising due to the coupling of charge carriers with lattice vibrations, play a critical role in determining the

transport characteristics. Depending on the specific material and its structural and electronic configuration, different conduction mechanisms may dominate. These include: Band Conduction: In materials with sufficient carrier density and delocalized electronic states, conduction occurs through band-like motion [4]. In systems with localized states, carriers hop between these states, overcoming energy barriers [5]. This mechanism is often described by the small polaron hopping model, with resistivity expressed as: Variable Range Hopping (VRH): In disordered systems at low temperatures, electron hopping between non-nearest neighbours becomes dominant. These mechanisms highlight the interplay between the structural disorder, carrier localization, and thermal activation in oxides, leading to diverse electrical transport behaviours. This study focuses on understanding the conduction mechanisms in the ferromagnetic perovskite oxide, which exhibits insulating behaviour at room temperature and shows a temperature-dependent resistivity consistent with the VRH model [6]. The insights gained contribute to the broader understanding of electron-phonon interactions and transport

processes in perovskite oxides, offering valuable implications for their potential applications in advanced technologies [7].

Method

The polycrystalline powder was synthesized using the modified auto-combustion method. Precursors ($\text{Pr}(\text{NO}_3)_3 \cdot 6\text{H}_2\text{O}$, $\text{Fe}(\text{NO}_3)_3 \cdot 9\text{H}_2\text{O}$, and $\text{Mn}(\text{NO}_3)_2 \cdot 4\text{H}_2\text{O}$) were dissolved in stoichiometric ratios in distilled water. The solutions were mixed in a 1000 ml beaker in equal weights. The citric acid in appropriate amounts, was added to the mixture and stirred continuously. The colloid was combusted in air at 250 °C for 2 hours to produce precursors. Pre-calcination was done at 600 °C for 2 hours to remove all organic materials and nitrates. Calcination is done in the temperature range of 800-900°C for 12 hours with intermediate grinding. A PANalytical X'Pert powder diffractometer was used for structural analysis. Rietveld refinement was performed using GSAS software. Microstructural images were recorded using a JEOL JSM-5600LV Scanning Electron Microscope (SEM). Physical Property Measurement System (PPMS, Quantum Design Dynacool) used for electrical and magnetic measurements.

Discussion

Structural Properties

The X-ray diffraction (XRD) measurements were performed over a 2θ range of 10° to 90°. The diffraction pattern was analyzed using the Rietveld refinement method, and the simulated patterns are presented in figure 1(a). The refinement confirmed the orthorhombic structure with the Pbnm space group. The refinement yielded a good fit, with reliability factors, and. Scanning Electron Microscopy (SEM) images of the sintered pellet, recorded at a magnification of 15,000 \times and an accelerating voltage of 10 kV, are shown in figure 1(b). These images reveal that the sample exhibits a homogeneous microstructure [8].

Magnetic properties

The magnetic measurements in the temperature range of 2–380 K were carried out for various external magnetic field strengths according to the measurement protocols. The FC magnetization exhibited a sign reversal, becoming negative below a specific temperature when the applied field was 20 Oe, 1000 Oe (figure 2) and 1 kOe. For ZFC magnetization at 20 Oe, a similar sign reversal was observed at low temperatures, but this phenomenon diminished as the external field strength increased. At 10 kOe, the FC magnetization remained positive across the entire temperature range (figure 3) [8, 9].

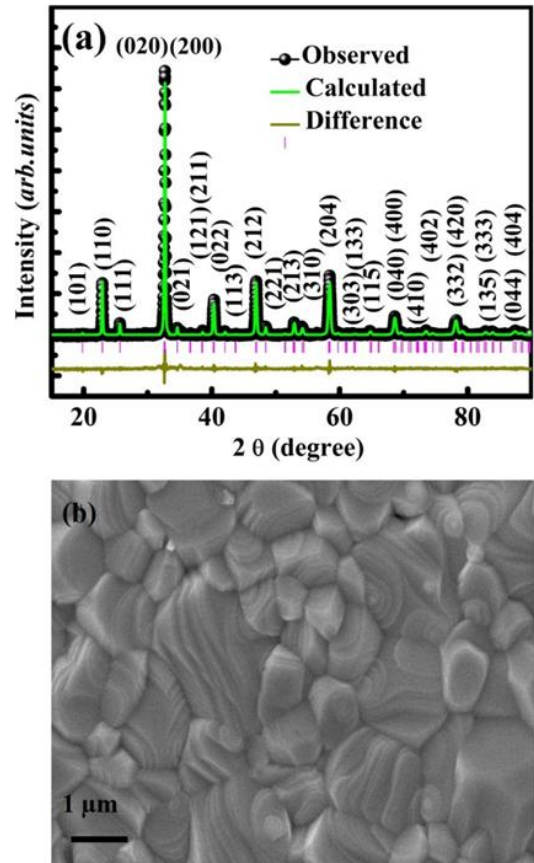


Figure 1: (a) XRD pattern of PFMO derived from Rietveld refinement within the 2θ range of 10° to 90°, and (b) SEM image of the sintered PFMO pellet captured at 10 kV with a magnification of x15000.

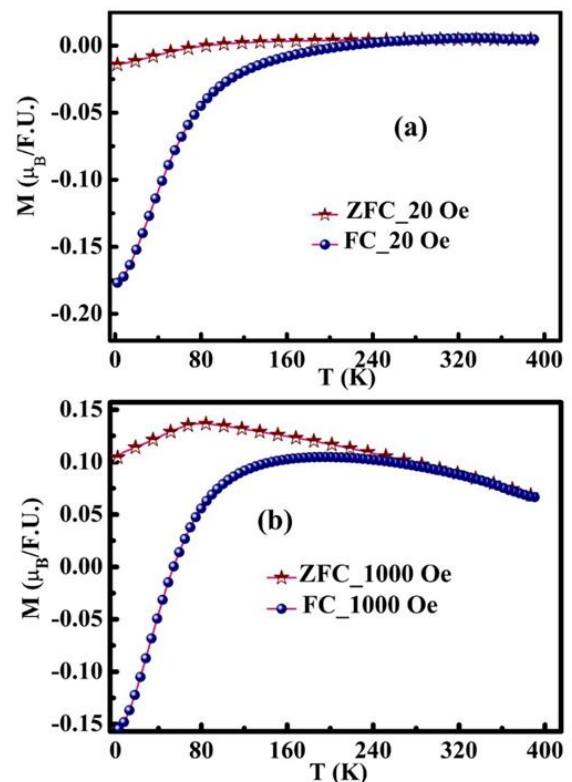


Figure 2: Dc magnetization measured at (a) 20 Oe, (b) 200Oe, (c) 1000Oe (d) and 10KOe at 2-380K.

In the FC process, as the temperature decreases, the magnetization also reduces. Upon further cooling, it sharply drops and becomes negative below a specific temperature known as the compensation temperature (T_{comp}). The M - T data at 20 Oe reveals a bifurcation between FC and ZFC magnetization at 213 K, where the magnetization becomes negative. As the applied magnetic field increases, the ZFC magnetization no longer shows a sign reversal, while the FC magnetization continues to exhibit negative values up to 1 kOe. Beyond this field strength, no sign reversal in magnetization is observed (Fig. 3(d)). The negative magnetization in different materials can be influenced by various factors, including artifacts like the trapped field from the superconducting magnet in the PPMS. To rule out such artifacts, the sign reversal of magnetization was verified through an FC field polarity test. For this test, FC measurements were conducted twice under magnetic fields of ± 500 Oe. When the sample was cooled from 380 K to 2 K under an external field of +500 Oe, the magnetization gradually increased, reaching a peak at 174 K. Subsequently, it decreased, crossing zero at $T_{\text{comp}} = 57$ K, and became negative, indicating that the magnetization direction opposed the applied field. Conversely, when a field of -500 Oe was applied, the magnetization showed a mirror-image behavior: it was negative at high temperatures but became positive below T_{comp} . This observation confirms that the negative magnetization in the material is not caused by the trapped field in the PPMS-VSM. Below the compensation temperature, negative magnetization is observed, especially at low magnetic fields, due to interactions between Fe ions and the paramagnetic contributions of Pr and Mn ions. [10].

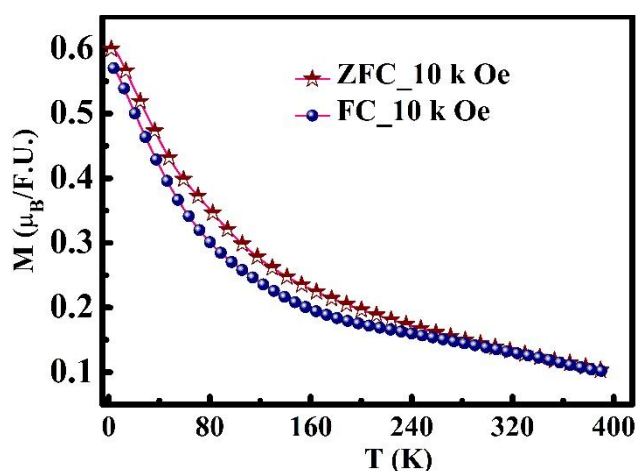


Figure 3: DC magnetization measured at 10kOe in the temperature range of 2-380K.

Electrical Properties

Materials are generally classified into three categories-

conductors, semiconductors, and insulators-depending on their behavior in response to an electric field. The concept of energy bands, which defines the range of energies an electron can occupy, is fundamental to understanding a material's electrical conductivity. These energy bands include the conduction band and the valence band. In insulators, the valence band is fully occupied, while the conduction band remains empty, separated by a significant energy gap [11]. In contrast, conductors allow an electric current to pass through effortlessly because their conduction band overlaps with the valence band, effectively eliminating any band gap. Semiconductors occupy an intermediate position, with their electrical conductivity falling between that of insulators and conductors. In semiconductors, the valence band is almost full, and the conduction band is nearly empty, with a relatively small energy gap of about 1 eV. Their band structure and atomic interactions largely influence the electrical behavior of these materials [12, 13].

In transition metal oxides, the conduction band is predominantly composed of oxygen 2p orbitals and metal d orbitals. The transport properties in these materials are influenced by the directional properties of the p and d orbitals and the Coulomb interactions within the d orbitals. The outer d electrons play a key role in determining the electrical behavior of these compounds. Metal oxides with disordered double perovskite structures are usually insulators, where the hopping of charge carriers governs the conduction mechanism [14].

In insulators, the movement of electrons is slow, leading to distortions in the surrounding lattice. These distortions create quantized lattice structures known as polarons, which facilitate conduction through hopping. This hopping mechanism can involve either electrons or polarons and varies across different materials (figure 4). There are three primary mechanisms for polaron hopping, each illustrated in figures 5 and 6. The first mechanism is thermally assisted tunneling, where carriers transition from a lower energy state to a higher one with the aid of thermal energy. The second mechanism is temperature-independent tunneling, where carriers move between states of equal energy without being influenced by temperature. The third mechanism involves carriers transitioning from a higher energy state to a lower one, accompanied by photon emission. Figure 5 highlights the three mechanisms of polaron hopping, labeled as (i), (ii), and (iii). Specifically, the mechanisms are as follows: (i) thermally assisted tunnelling, where carriers hop from a lower energy state to a higher energy state, (ii) temperature-independent tunnelling, where carriers hop between states of equal energy, and (iii) temperature-independent tunnelling, where carriers move from a higher energy state to a lower energy state, accompanied by photon emission [15]. Several models describe the hopping

conduction mechanism, including the Arrhenius thermal activation conduction or bandgap model (TAC), nearest-neighbour hopping or small polaron hopping (NNH/SPH), and Mott's variable range hopping model (Mott-VRH). In the Arrhenius TAC model, the resistivity follows the Arrhenius law: $\rho = \rho_0 \exp\left(\frac{E_A}{k_B T}\right)$ where ρ_0 is a constant, E_A is the activation energy.

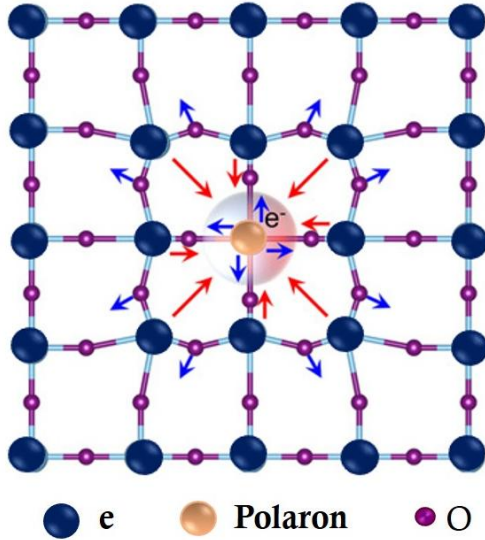


Figure 4: Polaron formation and conduction happening in perovskite structure.

VRH follows the equation, $\rho = \rho_0 \exp\left(\frac{T_0}{T}\right)^{1/4}$ where ρ_0 and

T_0 are constants. The equation, $N(E_F) = \frac{24}{\pi k_B T_0 \epsilon^3}$,

representing the density of localized charge carriers, where ϵ is the percolation length of the localized wave function. At higher temperatures, sufficient thermal energy enables nearest-neighbour hopping of small polarons between localized donor and acceptor sites. The NN-SPH model is represented by an equation where $\rho = A k_B T \exp\left(\frac{E_A}{k_B T}\right)$.

Figure 6 illustrates the VRH and NN-SPH mechanisms [16].

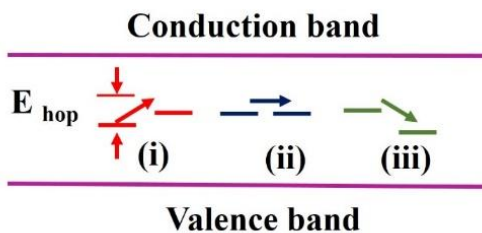


Figure 5: Electron /polaron hopping in insulating materials.

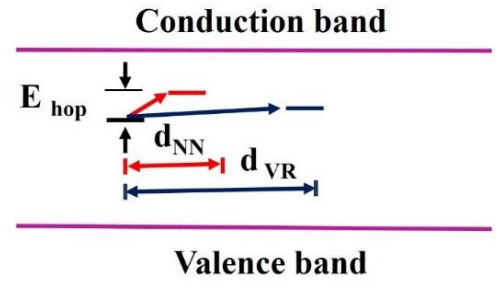


Figure 6: Mott's Variable range hopping polarons in perovskite materials.

In certain instances, the conduction process involves the combined contribution of both variable range hopping (VRH) and small polaron hopping (SPH) mechanisms. This cooperative behaviour, referred to as variable range hopping of small polarons (VR-SPH), can be mathematically described by integrating the respective equations for these two mechanisms.

$$\rho = B T \exp\left(\frac{E_A}{k_B T} + \left(\frac{T_0}{T}\right)^{1/4}\right)$$

where B is a constant.

Figure 7 (a) presents the resistivity (ρ) with temperature (122–300 K). At room temperature, PFMO exhibits insulating behaviour with a resistivity of approximately $4.1 \times 10^3 \Omega \text{m}$, which is aligned with previous reports. As the temperature decreases, the resistivity increases, reaching $73.47 \times 10^3 \Omega \text{m}$ at 122 K. A sharp rise in ρ is observed below 160 K, consistent with earlier reports. The resistivity in the temperature range of 2–300 K, as depicted in figure 7, adheres to the VRH model. The $\ln \rho$ vs. $1/T^{1/4}$ plot is shown in figure 7 (b). Parameters obtained after fitting (Red Line), $T_0 = 0.866 \times 10^9 \text{ K}$ and $\rho_0 = 40.42103 \Omega \text{m}$. $N(E_F) = 1.757 \times 10^{-25} \text{ eV}^{-1} \text{m}^{-3}$. Activation energy E_A ($E_A = \frac{k_B}{4} T_0^{1/4} T^{3/4}$) is calculated and observed as varying from 0.13 to 0.26 eV for 122 K to 300 K [6].

Disorder-induced localization of charge carriers in transition metal oxides plays a crucial role in determining the hopping conduction mechanism, as described by Mott's theory [17]. In $\text{Pr}_2\text{FeMnO}_6$, Fe/Mn site disorder and oxygen vacancies significantly influence the density of localized states near the Fermi level, affecting electrical transport. Cationic disorder at the Fe/Mn sites disrupts hybridization between B-site transition metals and oxygen, reducing the effective hopping integral and favouring polaronic conduction [18]. Similarly, oxygen vacancies act as electron donors, introducing localized states that facilitate hopping transport, as observed in $\text{La}_{1-x}\text{Sr}_x\text{MnO}_3$ [19]. Our resistivity

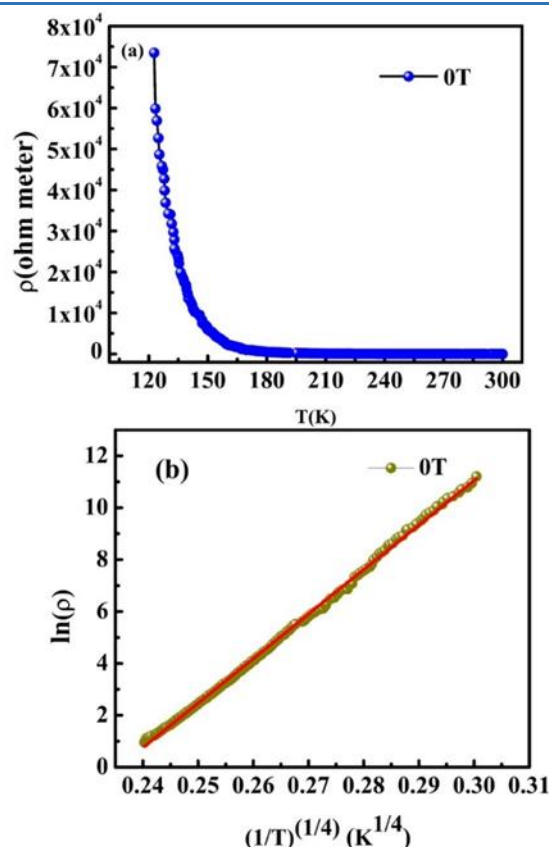


Figure 7: (a) Temperature-dependent resistivity, and (b) resistivity fitted using the VRH model.

data follows the Mott VRH model, indicating that charge carriers hop between localized states at different energy levels. The extracted hopping parameters, such as localization length and density of states near the Fermi level, align with previous reports on perovskite oxides exhibiting polaronic conduction. These findings suggest that disorder-induced localization in $\text{Pr}_2\text{FeMnO}_6$ is a dominant factor in its transport behaviour [20]. Our analysis provides a broader understanding of how structural disorder impacts VRH conduction, reinforcing the significance of disorder-driven transport mechanisms in $\text{Pr}_2\text{FeMnO}_6$. Many double perovskites, such as $\text{La}_2\text{NiMnO}_6$, $\text{Gd}_2\text{NiMnO}_6$ and $\text{Sm}_2\text{FeMoO}_6$, exhibit polaronic transport, but the degree of disorder and electron-phonon coupling varies significantly across different systems [21, 22]. In $\text{La}_2\text{NiMnO}_6$, the transport mechanism is influenced by Ni/Mn cation ordering, which determines the balance between metallic and insulating phases. In contrast, $\text{Sr}_2\text{FeMoO}_6$ displays a unique interplay between spin-polarized transport and disorder-driven localization, which differs from the strong polaronic hopping seen in $\text{Pr}_2\text{FeMnO}_6$. Our study demonstrates that in $\text{Pr}_2\text{FeMnO}_6$, Fe/Mn site disorder and oxygen vacancies play a dominant role in the VRH mechanism, making its conduction behaviour distinct from these related systems. Unlike $\text{La}_{1-x}\text{Sr}_x\text{MnO}_3$, where hole doping tunes the transport from insulating to metallic $\text{Pr}_2\text{FeMnO}_6$ remains insulating due to

stronger carrier localization effects. The activation energy and hopping parameters extracted from our data also suggest stronger electron localization than in many previously studied perovskites, reinforcing the novelty of our findings. This comparative analysis places our results within the broader context of perovskite transport studies and further validates the distinct nature of VRH conduction in $\text{Pr}_2\text{FeMnO}_6$.

Conclusion and Future Prospective

The double perovskite PFMO was synthesized using the citrate-gel combustion method. This compound adopts an orthorhombic crystal structure belonging to the Pbnm space group. Below the compensation temperature, negative magnetization is observed, especially at low magnetic fields, due to interactions between Fe ions and the paramagnetic contributions of Pr and Mn ions. The anomaly associated with the compensation temperature is examined using established theoretical models. Electrical transport studies indicate that PFMO behaves as a semiconductor, with its conduction governed by the VRH mechanism. The resistivity data within the 122–300 K temperature range conform to the VRH model, while the density of charge carrier states confirms the dominance of localized states in transport properties. These findings emphasize the material's semiconducting nature and offer important insights into its charge transport behavior.

References

1. Y. Moritomo, A. Asamitsu, H. Kuwahara, Y. Tokura, *Giant magnetoresistance of manganese oxides with a layered perovskite structure*, Nature, 380 (1996) 141-144.
2. A. Maignan, V. Caignaert, C. Simon, M. Hervieu, B. Raveau, *Giant magnetoresistance properties of polycrystalline praseodymium-based manganese perovskites: from $\text{Pr}_{0.75}\text{Sr}_{0.25}\text{MnO}_{3-\delta}$ to $\text{La}_{0.75}\text{Sr}_{0.25}\text{MnO}_3$* , Journal of Materials Chemistry, 5 (1995) 1089-1091.
3. T. Goto, T. Kimura, G. Lawes, A. Ramirez, Y. Tokura, *Ferroelectricity and giant magnetocapacitance in perovskite rare-earth manganites*, Physical review letters, 92 (2004) 257201.
4. C. Ganeshraj, R.N. Mahato, D. Divyaa, P. Santhosh, *Magnetic, electrical transport and structural investigations of orthorhombic perovskite $\text{Pr}_2\text{MnFeO}_6$* , Journal of Applied Physics, 107 (2010).
5. R. Ang, Y. Sun, Y. Ma, B. Zhao, X. Zhu, W. Song, *Diamagnetism, transport, magnetothermoelectric power, and magnetothermal conductivity in*

- electron-doped $\text{CaMn}_{1-x}\text{V}_x\text{O}_3$ manganites*, Journal of applied physics, 100 (2006).
6. R. Laiho, K. Lisunov, E. Lähderanta, V. Stamov, V. Zakhvalinskii, *Variable-range hopping conductivity in $\text{La}_{1-x}\text{Ca}_x\text{MnO}_3$* , Journal of Physics: Condensed Matter, 13 (2001) 1233.
 7. K. Aswathi, J.P. Palakkal, P.N. Lekshmi, M.R. Varma, *A Griffiths-like phase and variable range hopping of polarons in orthorhombic perovskite $\text{Pr}_2\text{CrMnO}_6$* , New Journal of Chemistry, 43 (2019) 17351-17357.
 8. K. Aswathi, J.P. Palakkal, M. RaamaVarma, *Magnetization sign reversal, exchange bias, and Griffiths-like phase in orthorhombic perovskite $\text{Pr}_2\text{FeMnO}_6$* , Journal of Magnetism and Magnetic Materials, 476 (2019) 45-53.
 9. K. Aswathi, J.P. Palakkal, R. Revathy, M.R. Varma, *Sign reversal of magnetization in $\text{Sm}_2\text{CrMnO}_6$ perovskites*, Journal of Magnetism and Magnetic Materials, 483 (2019) 89-94.
 10. A. Kumar, S. Yusuf, *The phenomenon of negative magnetization and its implications*, Physics Reports, 556 (2015) 1-34.
 11. A. Tiwari, K. Rajeev, *Electrical transport in*, Journal of Physics: Condensed Matter, 11 (1999) 3291.
 12. N. Tsuda, *Electronic conduction in oxides*, Springer Science & Business Media, 2000.
 13. S. Khadhraoui, A. Triki, S. Hcini, S. Zemni, M. Oumezzine, *Variable-range-hopping conduction and dielectric relaxation in $\text{Pr}_{0.6}\text{Sr}_{0.4}\text{Mn}_{0.6}\text{Ti}_{0.4}\text{O}_{3\pm\delta}$ perovskite*, Journal of magnetism and magnetic materials, 371 (2014) 69-76.
 14. M. Javed, A. A. Khan, J. Kazmi, N. Akbar, S.N. Khisro, A. Dar, A. D. K. Tareen, M. A. Mohamed, *Variable range hopping transport and dielectric relaxation mechanism in GdCrO_3 rare-earth orthochromite perovskite*, Journal of Rare Earths, 42 (2024) 1304-1316.
 15. Y. K. Vekilov, Y. M. Mukovskii, *Variable range hopping conductivity in manganites*, Solid state communications, 152 (2012) 1139-1141.
 16. F. Zheng, L.-w. Wang, *Large polaron formation and its effect on electron transport in hybrid perovskites*, Energy & Environmental Science, 12 (2019) 1219-1230.
 17. N. F. Mott, E. A. Davis, *Electronic processes in non-crystalline materials*, OUP Oxford, 2012.
 18. D. Serrate, J. De Teresa, P. Algarabel, C. Marquina, J. Blasco, M. Ibarra, J. Galibert, *Magnetoelastic coupling in $\text{Sr}_2(\text{Fe}_{1-x}\text{Cr}_x)\text{ReO}_6$ double perovskites*, Journal of Physics: Condensed Matter, 19 (2007) 436226.
 19. L. Zhang, D.J. Singh, M.-H. Du, *Density functional study of excess Fe in Fe_{1+x}Te : Magnetism and doping*, Physical Review B—Condensed Matter and Materials Physics, 79 (2009) 012506.
 20. Y. Tokura, *Critical features of colossal magnetoresistive manganites*, Reports on Progress in Physics, 69 (2006) 797.
 21. A.K. Biswal, *Exploring the Physics and Application of biphasic $\text{La}_2\text{NiMnO}_6$ based Double Perovskites*, in, 2016.
 22. S. Anirban, A. Dutta, *Structure, small polaron hopping conduction and relaxor behavior of $\text{Gd}_2\text{NiMnO}_6$ double perovskite*, Journal of Physics and Chemistry of Solids, 159 (2021) 110292.